Christopher Chattman

Enhanced Conductivity of Cu Foam via Graphene Deposition

Faculty Sponsors

Dr. Stephen Wayne & Dr. Jerry Marchetta

Abstract

Metallic foams hold promise as a class of materials to address challenging applications where increased surface area and/or reduced weight is needed. The presence of high-volume open cell porosity can reduce strength and thermal conductivity. In this study, high conductivity graphene was deposited onto copper foam with the goal of increasing electrical and thermal conductivity beyond that of pure copper. Immersing the Cu-foam into an alcohol solution of dispersed graphene was found to be an effective method that led to increased electrical conductivity; however, the conductivity was found to be dependent upon the number of immersion cycles. The bending stiffness of the foam specimens was also measured, and an increase of about 30% was attained for graphene-coated specimens. These findings indicate that graphene coated metallic foams may, for instance, become suitable materials for space applications where high conductivity, low weight and structural rigidity are needed.

Nomenclature

A	ampere for current
V	voltage
Ω	units for resistance, ohm
S/m	units for electrical conductivity, Siemens per meter
$g/cm3$	units for density
κ	thermal conductivity, W/mK
σ	electric conductivity
T	absolute temperature, K
e	carrier charge
L	Lorenz number
k_b	Boltzmann constant

Introduction

Metallic foams have found wide application as chemical filters, sensors, supercapacitors, lightweight structural panels and heat exchangers due in part to the large surface area created by interconnected porous structures. Commercially available foams made from aluminum or copper are readily available and can be sandwiched to form lightweight, stiff composite-clad metal plates. Metal foams have inherently high structural stiffness-to-mass ratio making them attractive materials for lightweight construction.[1] Bonding the foam between two dense metal sheets creates a composite sandwich material, whose properties depend on the bond strength and the foam and outer sheet metal properties. The result is a lightweight high-stiffness panel since the foam is much stiffer than an outer sheet of the same mass. The Ariane 5 rocket cone prototype demonstrated the use of aluminum foam sandwich material for aerospace applications.[1] Conceptually, such foam plates may be suitable for satellite applications where weight savings is a critical aspect of launch costs. Once in space, thermal management becomes a key factor. The ability of metallic foam panels to efficiently transfer heat

could open new possibilities for high performance cube satellites. CubeSats generate internal heat from power supplies and other surface mounted electronics, which must be rejected by conduction through body panels, that in turn, radiate the heat into deep space from outer panel surfaces. The present study is aimed at addressing the challenge of increasing the thermal conductivity of metallic foams with graphene, which has roughly an order of magnitude higher thermal conductivity when compared to other metals. The Wiedemann-Franz law[2] provides a direct relationship between the electrical conductivity and the thermal conductivity of metals which is shown in equation 1:

$$L=\kappa/(\sigma T) = (\pi^2/3)(k_b/e)^2 \approx 2.44*10^{-8}\ W\Omega/K^2 \qquad (1)$$

where κ is thermal conductivity, σ is electric conductivity, T is absolute temperature, e is a carrier charge (electron charge), L is known as the Lorenz number and k_b is the Boltzmann constant. Since the measurement of electrical conductivity/resistivity is straightforward, we use that as the basis for comparative measurements of graphene coated metal foam performance.

Numerous studies have evaluated the role of foam characteristics, such as size and number of pores, on electrical conductivity. Cuevas et al. studied the relationship between porosity and electrical conductivity in open and closed cell metal foams and found that both four-point probe and eddy current methods produced similar results for closed cell foams.[3] The relative conductivity of open cell foams measured by different authors was, however, quite different. In general, they identified that for a fixed porosity, a smaller pore size led to a lower electrical conductivity. Larger pore sizes led to a better-bonded structure, resulting in higher electrical conductivity. Dharmasena and Wadley studied the electrical conductivity of open-cell aluminum foam (commercially available as Duocel) and found that conductivity had a linear dependency on the relative density (porosity) ranging from 4-12%.[4] They used the four-point probe method and pointed out that the orientation of the unit cells with respect to current flow direction was random. Apparent electrical conductivities of Duocel aluminum foam ranged from 0.95 to 3.33x106 S/m for relative densities ranging from 0.04 to 0.12, respectively. Further model studies of aluminum foam thermal conductivity were carried out with fluid saturating the foam porosity. Boomsma and Poulikakos found that when the solid conductivity was markedly higher than the fluid, increases in the effective thermal conductivity were best made by manipulating the foam solid structure, which governed the thermal conductivity even at a very high porosity.[5] In the present research, the contribution of graphene is critical, and we have identified literature

concerning the electrical and thermal properties of flake, self-assembled and CVD 2D and 3D graphene structures. The thermal conductivity of partially suspended single-layer graphene was measured by Nika et al. and found to be in the range of ~3000-5000 W/mK, depending on the graphene flake size.[6] Others have isolated and studied the thermal conductivity of graphene flakes in comparison to bulk graphite. Nika et al.'s modeling efforts showed that the thermal conductivity of graphene grows with the increasing linear dimension of the graphene flakes and can exceed that of the basal planes of bulk graphite when the flake size is in the order of a few micrometers.

Their findings provide insight for applications such as lateral heat spreaders and interconnects for nanoelectronic circuits.[7] Electrospray printing of graphene oxide nanoflakes, at room temperature using a shadow mask, was used by Taylor and Velásquez-García to create low-cost gas sensors. This additive manufacturing approach deposited graphene oxide onto SiO2-coated Si substrates to create sensors for relative humidity and ammonia.[8] The assembly of graphite oxide single layers was studied by Cote, Kim and Huang, who found that stable monolayers could be obtained without the need for surfactants or stabilizing agents due to the strong electrostatic repulsion between the 2D confined layers.[9] They also reported that the graphite oxide monolayers could be chemically reduced to graphene for electronic applications. Graphene oxide self-assembly was studied by Putz et al. who described three proposed mechanisms for the formation of graphene oxide: (i) highly ordered layering, (ii) semi-ordered accumulation and (iii) disordered concentration. These were characterized by the ordered stacking of graphene oxide sheets, the formation of loose aggregate, or by forced alignment of the nanosheets.[10] The Ultrasonic assisted self-assembly of monolayer graphene oxide was studied by Chang in the production of field effect transistor (FET) devices for detection of E. coli bacteria.[11] The FET was fabricated by the self-assembly of graphene oxide sheets on the device electrodes, with sonication of the concentrated graphene oxide immersion solution. They found that their electrostatic self-assembly method, with assistance of sonication, formed stable, uniform devices over a large area without aggregation, whereas without sonication, they formed folded or multilayered graphene oxide films.

The creation of graphene composites and 3-D graphene structures have led to promising new material configurations with significant improvements in conductivity. Graphene foam composites have also been shown to be effective as electromagnetic interference (EMI) shielding for electronic applications by fabricating an ultralightweight, highly conductive graphene-polymer foam composite. Chen et al.'s graphene polymer-foam composite had a density of 0.06 g/cm3 and was very effective in EMI

shielding in the 30 MHz – 1.5 GHz frequency range far surpassing the best metals and carbon-based composite materials.[12] The thermal properties of an electrically conductive thermal interface material (a hybrid graphene with metal particle filler), was studied by Goyal and Balandin over the temperature range of 300 to 400 K. These authors found that the thermal conductivity of the composites was increased by 500% with a relatively small graphene loading of 5-vol%.[13] Advanced electronic applications for graphene foam have been studied by Dong et al., who synthesized a hybrid structure of zinc oxide (ZnO) on three-dimensional graphene foam for electrochemical sensors and supercapacitor applications.[14] These authors recognized that CVD-grown 3D graphene provides a highly conductive continuous network, and that hybridizing them with other functional nanomaterials would open new routes for the applications of graphene materials.

Wintterlin and Bocquet reviewed the literature pertaining to graphene on metal surfaces of Co, Ni, Ru, Pt and Pd with a focus on how the graphene layers interact with the metal. Their detailed analysis showed that there was great variability in the interaction of the graphene film with the underlying metals, which was not well understood. They identified interactions ranging from pure physisorption to a relatively strong chemisorption, with Cu, Ag and Au interacting weakly.[15] Tynan et al. studied the synthesis of 3D metal graphene foams using a soft template procedure, a 4-step process whereby a metal/dextran gel is annealed to form a metal oxide foam, then exposed to methane chemical vapor deposition (CVD), producing a metal graphene foam which is then washed in acid resulting in graphene foam. Graphene sheets of various thickness and layers were realized.[16] Chen et al., employing a template directed CVD process, accomplished the direct synthesis of three-dimensional foam-like graphene macrostructures. The 3D foam consists of an interconnected flexible network of graphene that serves as the fast transport channel of charge carriers for high electrical conductivity.[17] Nine et al. describe graphene interlayer interactions and molecular bonds, which are principally responsible for initiating self-assembly of graphene sheets and creating complex structures with one-, two- and three-dimensional morphologies. Numerous self-assembly methods and self-assembled superstructures including fibers, thin films, spheres, crumpled particles, aerogel/hydrogels and honeycomb are discussed.[18] The significance of self-assembly is in producing a conductive layer, or path, allowing for easy heat transfer between, for instance, the inside of a cube satellite to the outside space environment.

The current study had the goal of improving electrical and thermal conductivity of Cu-metal foam (thru the Wiedemann-Franz law) by using graphene to infiltrate and coat the Cu-foam porous structure. Simple

immersion techniques were employed to accomplish graphene deposition onto Cu-foam with the intent of demonstrating a scalable, low-cost and easy-to-implement method. The results are organized by microscopic inspection of the coated and uncoated Cu-foam specimens, their electrical conductivities, and their mechanical stiffness.

Materials and Methods

The materials used in the study were commercially obtained open-cell copper foam and highly conductive graphene, whose composition and physical properties are listed in Table 1.

Material	Composition Wt. %	Thermal Conductivity W/mK	Density g/cm^3
Cu foam	99.90% Cu	-	0.413
Graphene	C > 98%	3,000 - 5,000 *	0.03 - 0.1 **

Table 1. Composition and measured properties for copper specimens used in the study. * indicates single layer graphene,[19] ** indicates graphene nanoplatelets.[20]

Specimens were prepared for measuring electrical conductivity and resistivity according to ASTM standards using a Lavolta DC power supply and a Fluke 115 multimeter. Due to limited availability of Cu-foam material the specimen geometry used was 90 mm x 10 mm x 1.6 mm. The four-point method was used in measuring the resistivity of the foam.[21] By varying the current on the power supply, voltage measurements were taken to determine resistance, then resistivity and conductivity. Thermocouples were used to monitor the temperatures of the specimens before and after testing to ensure they were at room temperature 293 K (68°F). For all Cu-foam specimens, the multimeter was placed in three different positions along the length of the foam, as indicated in Fig. 1. The initial position had the multimeter probes 1 cm apart from each other and 4 cm from the ends of the foam specimen. The spacing between the multimeter probes was held constant while shifting to the left and right 0.5 cm from the initial position taking measurements in three different locations to determine resistivity. One important aspect of this method is that one must maintain the horizontal and vertical displacements or else the voltage across the foam specimen may vary. The uncoated foam measurements became benchmarks for the coated specimen.

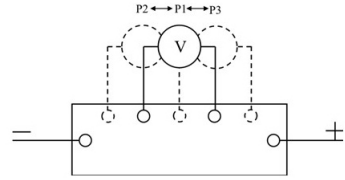

Figure 1. Rectangular foam specimen geometry.

The method used to coat the copper foam was simple immersion. Two sequences involved dipping the specimens, and a third had the specimen submerged until the solution completely evaporated (herein named 'sub-evap' specimens). The dipping experiments were controlled by using a CNC positioning device where the vertical (or z-axis) arm was programed to move down and up at a rate of 12.7 mm/min for 20 dips. The dipping solution was prepared in a 100 mL bottle using ethanol with a graphene concentration of 5% by weight then sonicated for one hour, following somewhat the method put forth by Chang et al.[11] After sonication, the bottled solution was placed onto the CNC stage with the copper foam specimen just above. To ensure complete submersion, the length of the foam had to be less than the depth of the solution. The specimen was dipped 10 times before electrical measurements were made, and another set of measurements at 20 total dip cycles. The sub-evap specimen procedure placed the foam specimen in the graphene solution while leaving the bottle open to allow the ethanol to evaporate and the graphene to settle and dry onto the foam.

Microscopic inspection of copper foam specimens was carried out using a Keyence light microscope. The bending stiffness of the Cu-foam specimens was carried out using an IMass TL-2300 instrument, that was adapted to measure the bending force of the end-clamped Cu-foam beams with an 80 mm unsupported length. The device recorded force (g) versus displacement (mm) and was programmed to move 36mm at a rate of 5 mm/s.

Results

Fig. 2a shows the uncoated Cu-foam as received. Fig. 2b is the sub-evap specimen surface showing that once the ethanol evaporated, the graphene in solution settled and deposited a relatively thick film of graphene over the surface. The ligaments of the foam became encased, including the pores which can be seen to be partially filled by the graphene. In fact, quantitative

analysis of the sub-evap specimen revealed that approximately 80% of the specimen surface was covered with graphene, as shown in Fig. 3a and Fig. 3b. Here, the reflective copper surface is enhanced and displayed in red. When it came to the dipping results in Fig. 2c, the graphene appears to have adhered onto the foam skeletal ligaments, rather than covering the pores, as was the case with sub-evap specimens. The dark regions in this image are deposits of graphene.

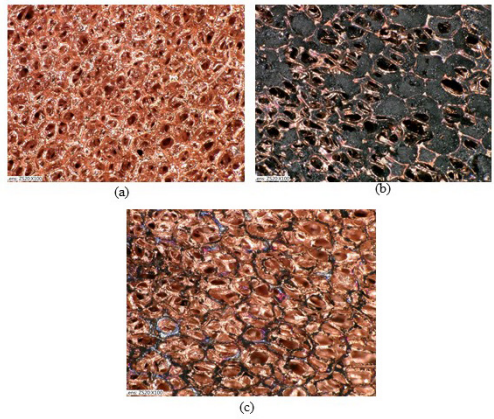

Figure 2. Light microscopy images of (a) Light micrograph of copper foam, as received, 100x magnification, (b) sub-evap specimen, 100x and (c) Light micrograph of copper foam, after 20 immersion cycles, 100x.

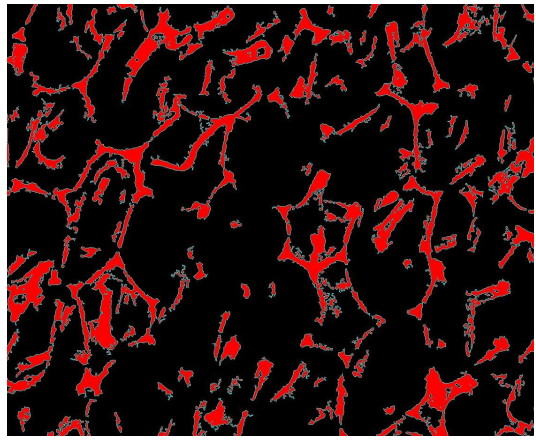

Figure 3a. Quantitative analysis of graphene by image contrast, sub-evap specimen, ZS20 Lens, 100x.

No.	Area	Perimeter	Max Diameter
1	2635.5960μm²	333.2247μm	100.8023μm
2	921.7183μm²	183.2679μm	52.9355μm
3	2805.8733μm²	491.3442μm	117.0308μm
4	2106.2558μm²	411.3908μm	111.6071μm
5	19774.3735μm²	1800.1844μm	313.7672μm
6	1410.4300μm²	235.3520μm	71.6019μm

No.	Area	Perimeter	Max Diameter
Average	4620.7319μm²	576.8414μm	134.0618μm
Standard Deviation	6685.1512μm²	664.4587μm	99.6457μm
Max	46755.9175μm²	5201.9388μm	565.0364μm
Min	740.3360μm²	132.3109μm	41.1299μm
Total	1437047.6232μm²	179397.6905μm	41693.2202μm

Total Area	1437047.6232μm²
Total Region Area	7107225.2142μm²
Area Ratio	20.2195%
Count	311 pcs

Figure 3b. Quantitative analysis of graphene by image contrast data, sub-evap specimen.

The immersion methods showed changes in conductivity; an increase of 3-13% in conductivity for the dipped specimen and an even higher increase when comparing the sub-evap results. The three measured positions are labeled as P1, P2, and P3 for the coated foam specimens. These were compared with the same three positions on an uncoated specimen. Table 2 presents the changes in the electrical conductivity with P3 having the greatest change for the dipped specimen and P2 for the sub-evap. The increased conductivity of the sub-evap specimen is attributed to the larger amount of deposited graphene. As coverage increased, so did the conductivity. The values obtained from all measurements are an average of 14 data points across three trials. Based on the data shown for dipped specimens, there is no apparent benefit for increasing the number of dips from 10 to 20.

	P1	P2	P3
Uncoated	19.9 ± 0.10	25.0 ± 0.10	25.0 ± 0.10
10 Dips	21.0 ± 0.17	26.2 ± 0.09	28.3 ± 0.12
20 Dips	20.8 ± 0.18	26.2 ± 0.11	27.9 ± 0.11
Sub-Evap	29.0 ± 0.49	50.7 ± 0.58	48.2 ± 0.57

Table 2. Electrical conductivity (S/m x 103) before and after dipping and immersion.

The sub-evap specimen results showed an increase in the stiffness of the foam, as compared to the uncoated specimens (Fig. 4). The slope of each line was taken to find modulus of elasticity, E, which is a measure of the material stiffness. The slopes were calculated to be 0.655 GPa for the uncoated and 0.858 GPa for the coated specimen. The bending stiffness of sub-evap specimen was in the order of 30% higher than the uncoated Cu-foam, no doubt a direct consequence of the graphene deposition.

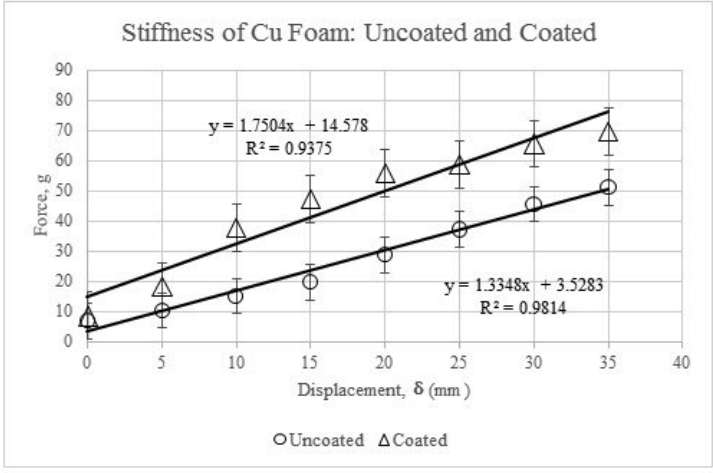

Figure 4. Plot of stiffness improvement after graphene deposition.

The trend lines in Fig. 4 are shown to have high R2 values meaning the stiffness curves are a good fit to the data. After 20 mm of displacement, some variation in bending force was observed for the sub-evap specimen and attributed to plastic deformation. Bending the coated specimen, the full

35 mm ensured permanent deformation and caused some graphene to flake off in regions where the highest bending stress occurred. While not shown, the stiffness measurements of the 10 and 20 dip cycled specimens were found to be equivalent to the uncoated specimen results shown in Fig. 4.

The calculated thermal conductivities (with respect to P2 from Table 2) were; 0.179 W/mK for the uncoated specimen, 0.187 W/mK for the 10 and 20 dips, and 0.362 W/mK for the sub-evap specimen. Based on these findings, the thermal conductivity of the sub-evap specimen was determined to be nearly twice that of uncoated Cu-foam.

Discussion

The goal of this study was to improve the electrical and thermal conductivity of Cu-metal foam by using high conductivity graphene to infiltrate and coat the Cu-foam porous structure. The graphene coating process chosen was economical and simple to execute by dipping the Cu-foam into a solution of ethanol with a graphene concentration of 5% by weight. This method led to variations in conductivity due to nonuniform graphene film deposition and is likely not the most optimal technique. More uniform coatings have been observed by CVD methods[14]. In order to achieve a highly conductive film of graphene, a high degree of graphene self-assembly is needed; there are a number of known alternative deposition techniques[17],[18]. Our coating method was shown to be capable of achieving ~80% coverage of the Cu-foam and that resulted in as much as a 50% increase in electrical conductivity as compared to uncoated foam, using our specific measuring techniques. The ability to measure thermal conductivity was not available at the time of this research and is considered an important measurement to understand the temperature sensitivity of the graphene coating. The possibility of improving the foam conductivity increases with full coverage and complete self-assembly of the graphene, so there is room for further improvement. In service, the Cu foam must have sufficient mechanical properties to be useful in electronic assemblies and to some degree also as a structural material. The bending stiffness of the graphene coated Cu foam was measured and shown to increase by 30% beyond that of uncoated material. This increase in modulus will translate to increased durability when handled and assembled into products. There is a great opportunity to create new high performance metallic foams through the integration of tailored coatings that, when combined, offer unique material properties for many engineering applications.

Conclusion

The electrical conductivity of pure copper foam and graphene-coated copper foam has been evaluated. It was found, by simple immersion of the copper foam into a sonicated solution of graphene flakes, that an adherent graphene film was deposited onto the copper foam. This resulted in an increase in electrical conductivity. The conductivity was found to be dependent upon the number of immersion cycles. Microscopic observations revealed that early in the dipping sequence, the electrically conductive network of graphene was established. A 22.5% increase in density was obtained and attributed to the filling of voids by graphene, resulting in a density of 0.506 g/cm3. This level of graphene infiltration also led to an increase in bending stiffness of about 30% for submersion-evaporated graphene coated specimens. These findings have shown that increases in electrical and thermal conductivity are possible by simple immersion deposition of graphene onto Cu-foam. These improvements offer promise for the future development of graphene coated metal foams as suitable materials for space applications where high conductivity and low weight are needed.

Acknowledgements

The authors gratefully acknowledge Barry Wymore for his technical support and two grants which provided funding for this study: The University of Memphis Faculty Research Grant and the NASA Tennessee Space Grant (NNX15AR73H).

References

[1] Banhart, J., and H-W. Seeliger. "Aluminium foam sandwich panels: Manufacture, metallurgy and applications." *Advanced Engineering Materials* 10.9 (2008): 793-802.

[2] Glazkov, V. N., L. Ginzburg, and A. Orlov. "Wiedemann-Franz law demonstration in a student practicum." *American Journal of Physics* 85.6 (2017): 473-477.

[3] Cuevas, F. G., et al. "Electrical conductivity and porosity relationship in metal foams." *Journal of Porous Materials* 16.6 (2009): 675.

[4] Dharmasena, K. P., and H. N. G. Wadley. "Electrical conductivity of open-cell metal foams." *Journal of Materials Research* 17.3 (2002): 625-631.

[5] Boomsma, K., and D. Poulikakos. "On the effective thermal conductivity of a three-dimensionally structured fluid-saturated metal foam." *International Journal of Heat and Mass Transfer* 44.4 (2001): 827-836.

[6] Nika, D. L., et al. "Lattice thermal conductivity of graphene flakes: Comparison with bulk graphite." *Applied Physics Letters* 94.20 (2009): 203103.

[7] Nika, D. L., et al. "Phonon thermal conduction in graphene: Role of Umklapp and edge roughness scattering." *Physical Review B* 79.15 (2009): 155413.

[8] Taylor, A. P., and L. F. Velásquez-García. "Electrospray-printed nanostructured graphene oxide gas sensors." *Nanotechnology* 26.50 (2015): 505301.

[9] Cote, L. J., F. Kim, and J. Huang. "Langmuir–Blodgett assembly of graphite oxide single layers." *Journal of the American Chemical Society* 131.3 (2008): 1043-1049.

[10] Putz, K. W., et al. "Evolution of order during vacuum-assisted self-assembly of graphene oxide paper and associated polymer nanocomposites." *Acs Nano* 5.8 (2011): 6601-6609.

[11] Chang, J., et al. "Ultrasonic-assisted self-assembly of monolayer graphene oxide for rapid detection of Escherichia coli bacteria." *Nanoscale* 5.9 (2013): 3620-3626.

[12] Chen, Z., et al. "Three-dimensional flexible and conductive interconnected graphene networks grown by chemical vapour deposition." *Nature Materials* 10.6 (2011): 424.

[13] Goyal, V., and A. A. Balandin. "Thermal properties of the hybrid graphene-metal nano-micro-composites: Applications in thermal interface materials." *Applied Physics Letters* 100.7 (2012): 073113

[14] Dong, X., et al. "Hybrid structure of zinc oxide nanorods and three dimensional graphene foam for supercapacitor and electrochemical sensor applications." *RSC Advances* 2.10 (2012): 4364-4369.

[15] Wintterlin, J., and M. L. Bocquet. (2009). Graphene on metal surfaces. *Surface Science*, 603 (10-12), 1841-1852.

[16] Tynan, M. K., et al. "Formation of 3D graphene foams on soft templated metal monoliths." *Nanoscale* 8.27 (2016): 13303-13310.

[17] Chen, Z., et al. "Three-dimensional flexible and conductive interconnected graphene networks grown by chemical vapour deposition." *Nature Materials* 10.6 (2011): 424.

[18] Nine, M. J., T. T. Tung, and D. Losic. "Self-Assembly of graphene derivatives: Methods, structures, and applications." *Comprehensive Supramolecular Chemistry II* 9.04 (2017): 47-74.

[19] Balandin, A. A., et al. "Extremely high thermal conductivity of graphene: Prospects for thermal management applications in silicon nanoelectronics." Silicon Nanoelectronics Workshop, 2008. SNW 2008. IEEE. IEEE, 2008.

[20] https://www.strem.com/uploads/resources/documents/graphene_nanoplatelets_copy1.pdf

[21] ASTM Standards: B193-16 Standard Test Method for Resistivity of Electrical Conductor Materials